RSC Advances

ROYAL SOCIETY OF CHEMISTRY

www.rsc.org/advances

Journal Name

ARTICLE

High Removal Performance of Dissolved Oil from Aqueous Solution by Sorption Process Using Fatty Acid Esterified Pineapple Leaves as Novel Sorbents

Received 00th January 20xx,
Accepted 00th January 20xx

DOI: 10.1039/x0xx00000x

www.rsc.org/

Siew Chin Cheu,[a] Helen Kong,[a] Shiow Tien Song,[a] Norasikin Saman,[a] Khairiraihanna Johari[b] and Hanapi Mat,[a,c*]

This paper demonstrates the potential use of lignocellulosic biomass of pineapple leaves (PAL) as oil sorbents by mercerization and esterification with long chain fatty acids in order to enhance its surface hydrophobicity and thus oil sorption capacity for treatment of dissolved oil contaminated wastewaters. The mercerized pineapple leaves (M-PAL) was esterified with lauric acid (LA) and stearic acid (SA) in pyridine/ p-toluenesulfonyl chloride (Py/TsCl) solution to yield M-LA-PAL and M-SA-PAL sorbents, respectively, which were then characterized against the raw PAL (R-PAL) sorbent using a scanning electron microscope (SEM), Fourier transform infrared (FTIR) spectroscopy, X-ray photoelectron spectroscopy (XPS), CHNS/O analyzer and Brunauer, Emmett and Teller (BET) surface area analyzer to study the changes of the surface morphology, functional groups, elemental compositions and specific surface area of the sorbents. It was found that the M-SA-PAL gave the highest sorption capacity (138.89 mg/g) followed by M-LA-PAL (107.67 mg/g) and R-PAL (35.59 mg/g), which are generally lower than dispersed oil sorption capacities. The oil sorption process was found to be exothermic in nature. The data analysis indicated that the sorption process obeyed the Langmuir isotherm and pseudo-second order kinetic models with film diffusion as the rate limiting step which was similar to some of the reported dispersed oil sorption results. The sorbent regeneration was repeated four times using the isopropanol-water (1:1, v/v) solution as a desorbing agent in which the sorption results were found to be comparable with the freshly prepared sorbent. Finally, the present findings indicate that the lignocellulosic biomass such as PAL could be a potential alternative as sorbent precursors for oil removal from oil contaminated wastewaters.

1. Introduction

The occurrence of oil no matter in effluent or water source is a worldwide concern which could lead to severe impact to humans and the environment. Oil contaminated aqueous solution mostly appears as small dispersed droplets and some even dissolved in water, make it hard to be removed and thus degrade the performance of the treatment plant [1,2]. In most circumstances the oily water is just discharged to the receiving environment, affecting the aquatic life survival and human economic activities [3]. Thus, the removal of oil and hydrocarbon contaminants from water is essential to preserve water for irrigation, livestock or wildlife watering and habitats as well as other industrial uses [2].

The removal of dispersed oil has gained considerable attention and in fact, several separation techniques are already available such as gravity separation, chemical treatment methods, flotation system, coagulation, filtration, hydrocyclone, and electrical process[2]. In contrast, less attention has been given on the dissolved oil separation from the water source. Generally, the removal of dissolved oil can be rather difficult than dispersed oil due to its solubility and low concentration. A combination of different techniques may be required to efficiently remove both forms of oil contaminants. Produced water from oil and gas exploration activities, for instance, consists of both oil contaminants, while groundwater contaminated by BTEX may consist of purely dissolved oil or hydrocarbons [4,5].

Among the main existing oil removal techniques, sorption process has gained high popularity as it is one of the easiest and most cost effective physiochemical methods to remove contaminants from aqueous solution. Synthetic organic polymers such as polypropylene, polyurethane and polyethylene have been widely used to remove oil. Synthetic polymers have high sorption capacity but their major drawbacks are non-biodegradability and high cost [6]. As a result, new research directions are being focused on developing low-cost sorbents derived from renewable and biodegradable materials such as lignocellulosic materials, however appropriate modifications are required in order to achieve acceptable sorbent technical specifications [7].

The pristine lignocellulosic materials mostly exhibit a lower oil sorption capacity than chemically modified ones due to the presence of hydroxyl group (OH) on their surfaces that tends to adsorb water more than oil. There are several modification methods that have been introduced for promoting interfacial adhesion in a system where lignocellulosic materials are used as fillers including acid treatment, alkaline treatment, etherification, esterification, polymer grafting and carbonization[8–15]. As a result, low-cost sorbents from different types of lignocellulosic materials to remove oil from water are also being widely studied such as

[a] Advanced Materials and Process Engineering Laboratory, Faculty of Chemical and Energy Engineering, Universiti Teknologi Malaysia, 81310 UTM Skudai, Johor, Malaysia.
[b] Department of Chemical Engineering, Faculty of Engineering, Universiti Teknologi PETRONAS, 32610, Bandar Seri Iskandar, Perak, Malaysia.
[c] Advanced Material and Separation Technologies (AMSET) Research Group, Health and Wellness Research Alliance, Universiti Teknologi Malaysia, 81310 UTM Skudai, Johor, Malaysia.
*Corresponding author. Tel.: +607-5535590; Fax: +607-558146; Email: hbmat@cheme.utm.my

kapok, sugarcane bagasse, rice husk, barley straw, oil palm fibers, and banana trunk fibers [1,14,16–20]. These studies are mainly focused on modifications of lignocellulosic materials for removal of dispersed oil, while the removal of dissolved oil by sorption process has hardly been reported, even though both forms of oil contaminants may co-exist in produced water and can be removed simultaneously during the sorption process. However, their sorption performance and mechanism can differ significantly to one another and studies towards fundamental understanding are thus crucial especially for the removal of dissolved oil since it has fewer research work over the dispersed oil contaminant.

In this study, lignocellulosic biomass of pineapple leaves (PAL) was used as sorbents for the removal of oil compounds from dissolved oil-in-water (o/w) solution. The PAL also has a high cellulose content (70-80 %) which could ease the modification processes due to the presence of high content of hydroxyl functional groups on their surfaces [11]. It was reported that the pineapple residue was previously used as a sorbent to remove cationic dyes (methylene blue and crystal violet) [21–24]. The PAL sorbents were prepared by mercerization and esterification of PAL under selected experimental conditions. The synthesized PAL sorbents were then characterized by using the scanning electron microscope (SEM), Fourier transform infrared (FTIR), X-ray photoelectron spectroscopy (XPS), and elemental analysis (EA) to study their morphological properties, surface functional groups and elemental compositions. The oil sorption performance of R-PAL, M-PAL, M-LA-PAL and M-SA-PAL sorbents was investigated at different experimental conditions and sorption experimental data were then analyzed using the existing equilibrium and kinetic models to understand the mechanism of dissolved oil sorption process. The results of this study will be useful towards the utilization of lignocellulosic biomass as low-cost sorbents in the removal of oil especially dissolved oil from wastewater.

2. Materials and experimental procedures

2.1 Materials

Pineapple leaves (PAL) were collected from Pekan Nenas (Johor, Malaysia). Chemicals such as fatty acids (lauric and stearic acid), pyridine, p-toluenesulfonyl chloride (TsCl), ethanol, methanol, isopropanol and acetic acid were purchased from Sigma-Aldrich (USA) and Merck (Germany). The crude oil used for the experiments was obtained from a local petroleum company. Double-distilled water was used for solution preparation throughout the experiments.

2.2 Sorbents preparation

The PAL was cut into small pieces and dried under sunlight for several days. The dried PAL were then ground into small sizes and sieved to obtain targeted sample size of 75-150 µm. The sieved PAL sample was soaked in ethanol and water mixture, followed by agitation and centrifugation to remove dirt and impurities. Then, the washed PAL sample was oven dried for 24 hours at 333 K and stored in a desiccator for further characterization and modifications. This PAL sample was referred to as raw PAL (R-PAL).

The R-PAL was then treated with 5 % (w/v) aqueous NaOH solution under constant stirring at room temperature (303 K) for 18 hours. The fibers were then washed with distilled water for several times to remove any traces of NaOH sticking on the fiber surface, neutralized with acetic acid and washed repeatedly with double-distilled water until pH 7. The product of the mercerization process was denoted as M-PAL.

The long chain fatty acids (lauric and stearic acids) modified M-PAL were synthesized in Py/TsCl system according to Jandura *et al.* [25]. An accurate weight of 5 g M-PAL was added to the 2-necked flask containing 150 mL of pyridine and 35 g of TsCl with continuous stirring and nitrogen purging for 20-30 minutes. The fatty acid was then added slowly into the mixture to give a 1:1 molar ratio. The mixture was maintained in an oil bath at a temperature of 60-70 °C and 80-90 °C for lauric and stearic acids, respectively, for 4 hours. The mixture was filtered and the solid product was washed with methanol followed by Soxhlet extraction using methanol for 18 hours to remove the excess fatty acid. The mixture was then filtered; washed with double-distilled water followed with acetone, and finally dried in an oven for 24 hours. The M-PAL modified by lauric and stearic acids was denoted as M-LA-PAL and M-SA-PAL, respectively.

2.3 Sorbent characterizations

The total content of carbon, hydrogen, oxygen and nitrogen was analyzed by using a CHNS/O analyzer (CHNS/O Analyzer 2400, PerkinElmer, USA). The surface morphology was determined using a scanning electron microscope (SEM) model JEOL JSM-7500F (Japan). The FTIR spectra were obtained using a FTIR spectrometer (Thermo Scientific, Nicolet iS5) via the ATR sampling technique and scanned over the range of 4000 to 400 cm^{-1} at a resolution of $4cm^{-1}$ to study the surface functional groups responsible for the oil sorption. The X-ray photoelectron spectroscopy measurement was carried out using a Shimadzu KRATOS AMICUS X-ray photoelectron spectrometer (XPS), equipped with unmonochromated aluminium Al Kα source (1486.8 eV) with an operating pressure of 10^{-9} mbar and 10 mA of current. The XPS spectra were taken at 150 eV of constant analyzer energy (CAE) mode with 1eV of energy step size, while high-resolution XPS spectra of O_{1s}, N_{1s} and C_{1s} were taken at 25eV of CAE and 0.05eV of energy step size. The specific surface area was measured by a Brunauer, Emmett and Teller (BET) surface area analyzer (Micromeritics ASAP 2000, USA) a using nitrogen adsorption-desorption method at -195.9ºC (77.3K).

2.4 Crude oil sorption experiment

A dissolved oil-in-water (o/w) solution was prepared by first dissolving a specific amount of crude oil in isopropanol, followed by dilution with double-distilled water to obtain the required oil concentration. In a typical sorption experiment, an accurate weight of PAL sorbent (i.e. 0.025 g) was added into a 50 mL conical flask containing 50 mL of 100 ppm of o/w solution. The flask was tightly fastened and placed in a temperature-controlled shaker at a speed of 200 rpm at a selected temperature to reach equilibrium. The sample was then withdrawn and filtered using a 0.8 µm syringe filter, and the filtrate (supernatant) was collected. The residual oil concentration in the supernatant was extracted using isooctane and analyzed using a UV-VIS spectrophotometer (PerkinElmer model Lambda 35) measured at 257 nm. All experiments were carried out in triplicate and an average value was reported. The sorption capacity of the sorbent at time t, q_t (mg/g) was calculated using the mass balance equation as in Eq. 1.

$$\text{Sorption capacity, } q_t = \frac{C_0 - C_t}{M} V \quad (1)$$

where C_o and C_t are respectively the oil concentrations at initial (t = 0) and time t (t = t) (mg/L), *M* is the sorbent mass (g), and *V* is the volume of the oil solution (L). The sorption capacity at equilibrium is denoted as q_e.

2.5 Crude oil composition determination

The content of crude oil in water solution was analyzed using a gas chromatography mass spectrometer (GC-MS) using a HP-5ms column (30 m x 0.25 mm x 0.25 µm). Helium was used as a carrier gas and the split injection mode was used. The injector and MSD transfer line heater temperature was set at 250°C and 290°C, respectively. The oven was programmed for an initial temperature of 40°C for 2 minutes, followed by heating at 5°C/min to 290°C and held for 10 minutes.

2.6 Sorbent regeneration studies

The regeneration experiments were conducted using oil-loaded sorbents (0.05g/L) prepared using 100 ppm crude oil in water (w/o) solution. The regeneration experiments were carried out by mixing oil-loaded sorbent with isopropanol-water (1:1, v/v) solution having the dosage of 0.05g/L and shaking at 200 rpm for 24 hours to ensure sufficient desorption time. The sorbent was then separated for the next cycle of sorption while the filtrate was extracted using isooctane and analyzed using a UV-VIS spectrophotometer measured at 257 nm to determine the desorbed oil concentration. The same procedures were repeated for the following sorption and desorption cycles.

3. Results and Discussions

3.1 Morphology and textural properties analysis

The most common and simple device to study the surface morphology of the solid samples is by using a scanning electron microscope (SEM). The surface morphologies of R-PAL, M-LA-PAL and M-SA-PAL sorbents at 10,000x magnifications are shown in Figs. 1(a), 1(b), 1(c) and 1(d), respectively. A regular and smooth surface can be observed for untreated PAL[26]. The mercerization treatment reduced the fiber diameter and increased the number of active sites available for further modification[11]. The mercerization and esterification process partially dissolved the soluble components (e.g. hemicellulose, lignin, and wax), made the fiber surface rougher and irregular [11,12]. The removal of a waxy cuticle layer of PAL also increased the contact surface area for oil sorption.

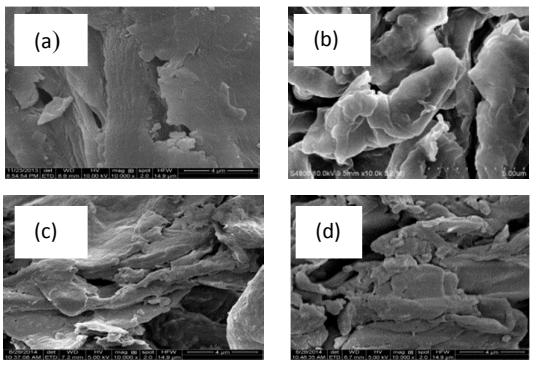

Fig. 1 SEM image of (a) R-PAL, (b) M-PAL, (c) M-LA-PAL, and (d) M-SA-PAL sorbents (Magnification: 1000x).

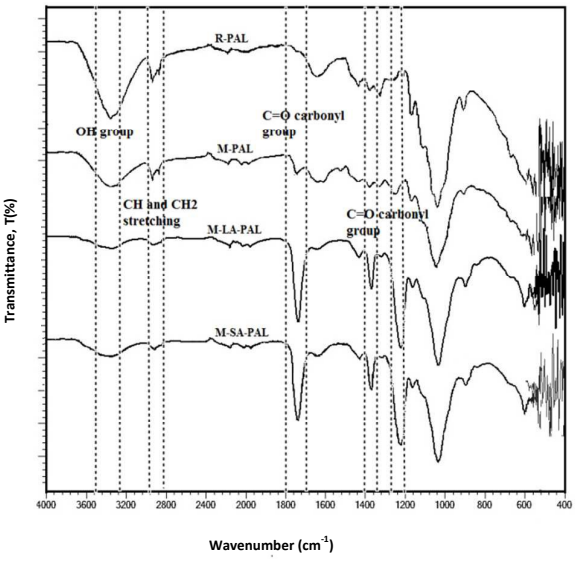

Fig.2 FTIR spectra for R-PAL, M-PAL, M-LA-PAL, and M-SA-PAL sorbents.

3.2 Functional groups identification

The surface functional groups of PAL sorbents before and after chemical modification were determined by examining FTIR spectra as shown in Fig. 2. The observed band at ~3340 cm^{-1} corresponded to the intermolecular and intramolecular hydrogen bonding in cellulose [8]. Two peaks observed at 2850-3000 cm^{-1} were identified as asymmetric C-H and C-H_2 groups stretching [27]. Peaks at ~1730 and ~1245 cm^{-1} corresponded to the presence of pectin [28]. A lignin peak was found at ~1631 cm^{-1} due to the C=C in-plane aromatic vibrations [28]. The cellulose was characterized by the peak at 1036 cm^{-1} [26].

The effect of mercerization and esterification was observed as the vibration peak intensity at ~1631 cm^{-1} decreased due to the decrease in the stretching vibration of lignin. This indicated that mercerization and esterification led to the partial removal of lignin [29]. Besides, the sharp peak at ~3340 cm^{-1} was broadened and less defined indicating that the fibers have lowered the hydrogen bonding with a change in the structure after the chemical modifications. The decrease in intermolecular hydrogen bonding indicated that the hydroxyl groups have been esterified by fatty acids. It was supported by the increment of the peak intensity of CH_2 and CH_3 groups and C=O stretching of carbonyl group (~1750 cm^{-1}) which also meant the successful grafting of lauric and stearic acids into the PAL surfaces after the treatment of PAL with fatty acids[8].

The XPS spectra of R-PAL, M-LA-PAL and M-SA-PAL are shown in Figs. 3(a), 3(b) and 3(c), respectively. The PAL sorbents mainly comprise of carbon and oxygen as main elements observed at 285 and 533 eV as they are from lignocellulosic material [30]. Fig. 4 (a) shows the analysis of the total C_{1s} high-resolution spectra of the raw and fatty acid modified PAL sorbents confirming that four component peaks found at 285.0 eV, 286.9 eV, 288.7 eV and 289.6 eV represented the C1(C-C/C-H), C2 (C-OH), C3(O-C-O, C=O), and C4 (O-C=O), respectively [13,31]. Meanwhile, Fig. 4(b) shows the O_{1s} high resolution spectra of the unmodified and fatty acid grafted PAL at peak 532.2 eV. The R-PAL was found to have abundant C1 and C2 in

Journal Name

ARTICLE

Table 1. Elemental compositions (wt. %) of R-PAL, M-PAL, M-LA-PAL, and M-SA-PAL sorbents.

	Composition (wt. %)				Atomic ratio	
Sorbents	**C**	**H**	**O**	**N**	**O/C**	**H/C**
R-PAL	43.06	6.184	48.976	0.98	1.1374	0.1436
M-PAL	41.71	6.50	47.09	0.15	1.1290	0.1558
M-LA-PAL	57.95	8.08	30.05	0.12	0.5186	0.1394
M-SA-PAL	63.08	9.15	24.36	0.11	0.3862	0.1451

the C_{1s} spectra indicated that the R-PAL mainly consists of lignin (plant wax in lignocellulose mainly contributes to C1), hemicellulose and cellulose[13]. After the esterification process, C4 group (carbon atoms bonded to a carbonyl and a non-carbonyl oxygen (O=C-O)) were found in M-LA-PAL and M-SA-PAL sorbents. It was observed that the peak intensity of O_{1s} spectra increased after the surface modification, proving that ester groups had been added to the PAL surfaces.

3.3 Elemental analysis

The elemental compositions of the PAL before and after fatty acid grafting are given in Table 1. The carbon and oxygen content decreased after the mercerization might be due to the removal of hemicellulose and lignin during the mercerization. Hemicellulose is water soluble as it is composed of a mixture of different sugars while lignin has components which are soluble in NaOH solution [29]. After the esterification, the composition of carbon in M-LA-PAL and M-SA-PAL was increased to 57.95 % and 63.08 %, respectively. There was also a drastic decrease in O/C atomic ratio from 1.1290 (M-PAL) to 0.5186 (M-LA-PAL) and 0.3862 (M-SA-PAL) after the esterification. This is due to the introduction of long chain alkyl group of lauric acid (12 carbons) and stearic acid (18 carbons) to the M-PAL surfaces.

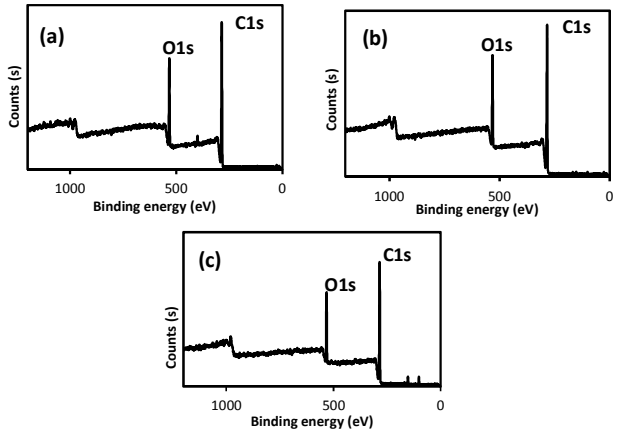

Fig. 3 XPS wide scans of (a) R-PAL, (b) M-LA-PAL, and (c) M-SA-PAL sorbents.

3.4 Effect of pH

The solution pH is a crucial parameter to be studied in sorption process as it affects the solute chemistry and surface binding sites of the sorbents[8,32]. The sorption of oil onto PAL sorbents as a function of solution pH was studied as shown in Fig. 5. It was observed that the oil sorption capacity was the highest at equilibrium pH of 7.07 observed for R-PAL (20.58 mg/g), 5.07 for M-LA-PAL (106.62 mg/g) and 5.30 for M-SA-PAL (148.85 mg/g). The oil sorption capacity of M-LA-PAL was found to decrease slightly with the increase of solution pH after the equilibrium pH of 5.07. The M-SA-PAL oil sorption capacity decreased rapidly to 116.55 mg/g at equilibrium pH of 6.81 and then decreased slightly with the increase of solution pH. This indicated that oil sorption process is more favorable in a slightly acidic to neutral condition. The increase of acidity and alkalinity to the oil solution may cause to the increase of the oil solubility indicating the decrease of hydrophobicity properties of the oil molecules. This leads to the decrease in the oil sorption onto hydrophobic M-LA-PAL and M-SA-PAL surface in highly acidic and alkaline solution. Besides, there is also possibility in reducing of sorbent hydrophobicity properties due to the existence of huge amount of protons that are localized on the sorbent surface at lower pH[33]. In an alkaline condition, the oil sorption capacity at high pH values in fact does not correspond to the oil removal efficiency. The addition of NaOH to the oil solution caused the saponification process to occur, where the oil underwent hydrolysis with NaOH to produce glycerol and fatty acid salts that are more soluble in water than isooctane solvent[8]. Thus, the final oil concentration determined was lower than it should be as the oil was hydrolyzed in the solution and not being extracted by the isooctane.

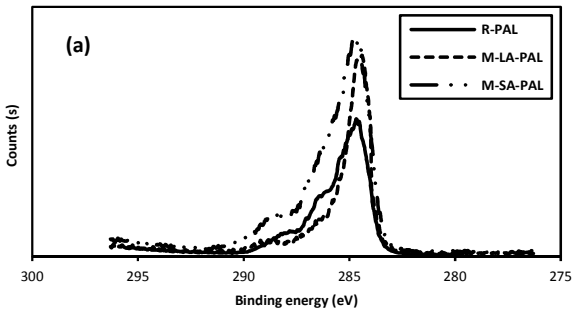

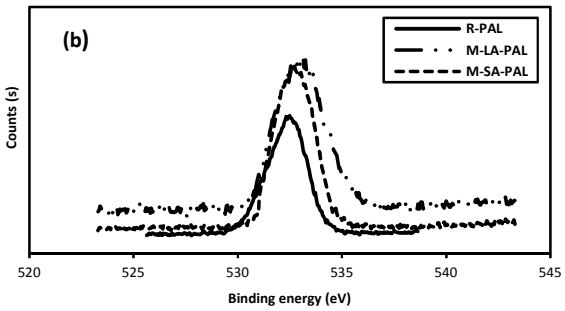

Fig. 4 XPS spectrum of (a) total C_{1s} high resolution spectra and (b) total O_{1s} high resolution spectra of the R-PAL, M-LA-PAL and M-SA-PAL sorbents

3.5 Effect of initial oil concentration

The study of initial oil concentration is important as it strongly affects the thermodynamics and kinetics of the adsorption process [34]. The effect of initial oil concentration on oil sorption capacity was studied by varying the oil concentration from 10 to 300 ppm, while other parameters such as sorbent dosage (0.5 mg/mL), contact time (24 hours) and temperature (303±0.5 K) were kept constant. Fig. 6(a) shows the relationship between initial oil concentration and the oil sorption capacity for R-PAL, M-LA-PAL, and M-SA-PAL. The experimental data show that the oil sorption capacity increases with oil concentration up to a certain level and attains equilibrium. This result may be due to the saturation of active sites of PAL sorbents by oil which hinders further oil adsorption onto the active sites. The low oil sorption capacity at the initial stage is due to the limitation of the oil molecules available for attachment on the sorbent surfaces. The maximum oil sorption capacity for R-PAL, M-LA-PAL and M-SA-PAL sorbents was 37.45, 182.47 and 198.93 mg/g, obtained at equilibrium concentration (C_e) of 63.97, 131.47 and 123.24 ppm, respectively followed the order of M-SA-PAL > M-LA-PAL > R-PAL. The modified PAL sorbents exhibited a higher sorption capacity than R-PAL due to the presence of hydrophobic group from a long chain fatty acid, thus enhancing the hydrophobic character of the sorbent surfaces. The M-SA-PAL shows the highest sorption capacity as the stearic acid has a longer carbon chain (18 carbons) as compared to the lauric acid (12 carbons) for the M-LA-PAL.

The sorption data were further analyzed using the existing isotherm models in order to study the distribution of the adsorbed molecules between the liquid and solid phases at the equilibrium state [35]. This is crucial towards a better understanding on the fundamental aspects of the sorption process and optimizing the use of sorbents in oil removal process [34]. The experimental data were thus fitted into three most commonly used sorption isotherm models, namely Langmuir, Freundlich and Temkin. The Langmuir isotherm was initially developed to describe the sorption of gas to solid surface. It assumes a monolayer sorption onto a homogeneous surface which contains a finite number of adsorption sites. The Freundlich isotherm is an empirical equation which represents the multilayer adsorption on heterogeneous surfaces that has non-uniform available sites with different energies of adsorption. The Temkin considers the effect of indirect sorbate/adsorbate interaction on sorption isotherm, due to the interaction, the heat of sorption of all the molecules in the layer would decrease linearly with coverage [35].

The linear forms of the Langmuir, Freundlich and Temkin isotherm models are given by Eqs. 2, 3, and 4, respectively.

$$\frac{C_e}{q_e} = \frac{1}{q_m K_a} + \frac{1}{q_m} C_e \quad (2)$$

$$\ln q_e = \ln K_F + \frac{1}{n} \ln C_e \quad (3)$$

$$q_e = B \ln A + B \ln C_e \quad (4)$$

where q_e is the oil sorption capacity at equilibrium time (mg/g), C_e is the oil concentration at equilibrium (mg/L), q_m is the theoretical maximum sorption capacity (mg/g), K_a is the Langmuir sorption constant, K_F and n are Freundlich constants respectively indicating the extent of the adsorption and the favorability of the sorption process, 1/n is the slope of the plot ranging from 0 to 1 is the measure of the surface heterogeneity, the closer the value to zero, the more heterogeneous the sorbent surface [14]. In Eq. 5, A is the Temkin isotherm equilibrium binding constant (L/g) and B (= RT/b_T) in which the b_T is the Temkin constant related to heat of sorption (J/mol), R is the gas constant (8.314 J/mol. K) and T is the absolute temperature (K).

The best-fitted isotherm model for R-PAL, M-LA-PAL and M-SA-PAL is shown in Fig. 6(b), while the model constant parameters, coefficient of determination (R^2) and Pearson's chi-squared test (χ^2) analysis are tabulated in Table 2. The χ^2 was determined according to Eq. 5.

$$\chi^2 = (q_{exp} - q_{cal})^2 / q_{cal} \quad (5)$$

where q_{exp} and q_{cal} refer to the experimental and calculated q, respectively. The best fitting model should have R^2 value of equal or near to 1, smaller value of χ^2, closer $q_{e,\,calc}$ value to that of the $q_{e,\,exp}$, and a good non-linear fitting, in which the Langmuir isotherm model meets the most of these criteria. This indicates that the oil sorption onto the PAL sorbents is a monolayer sorption. Similar results were reported for the sorption of dispersed/emulsified oil onto oil palm fiber, rice husk and barley straw surface indicating monolayer sorption[1,20,27].

3.6 Effect of temperature

Temperature has a direct influence on the sorption capacity of the sorbate onto any sorbents. It needs to be studied as it is a primary thermodynamic property that determines other properties such as ΔH, ΔS and ΔG. These thermodynamic properties are important to be evaluated in order to understand the nature of the sorption process. In the present study, the sorption experiments were conducted in the temperature range of 303-343 K, while other parameters were kept constant. As shown in Table 3, the sorption capacity of PAL sorbent decreases with the increase of temperature, indicating that the process is exothermic[8].

The performance of oil sorption as a function of temperature could be further evaluated by analyzing the thermodynamic parameters namely the Gibbs free energy (ΔG), enthalpy (ΔH) and entropy (ΔS). The change in Gibbs free energy (ΔG) of the sorption is calculated according to Eq. 6.

$$\Delta G = -RT ln K_c \quad (6)$$

where K_c is the sorption equilibrium constant, obtained by $K_c = q_e$ (sorbent)/C_e (solution) at the process temperatures of 303 K, 323 K and 343 K after 24 hours. The value of the enthalpy change (ΔH) and entropy change (ΔS) at constant temperature related to the

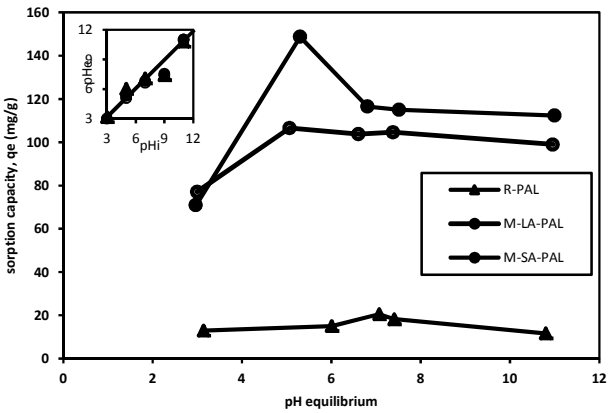

Fig. 5 Effect of pH on oil sorption onto PAL sorbents. Experimental conditions: pH, 3-11; oil concentration, 100 ppm; sorbent dosage, 0.5 mg/mL; t, 24 hours; and T, 303 K.

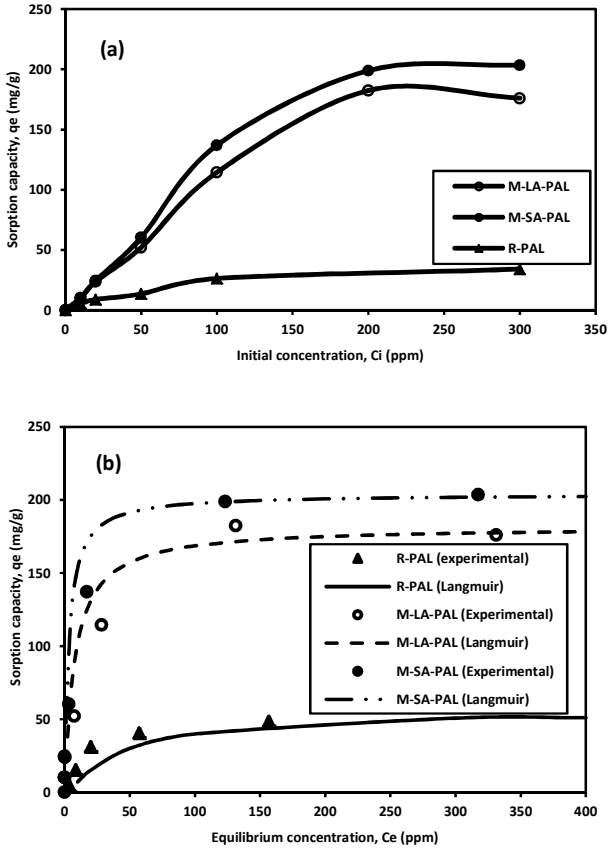

Fig. 6 Oil sorption onto PAL sorbents: (a) effect of initial concentration and (b) sorption isotherm. Experimental conditions: pH, 7; oil concentration, 10-300 ppm; sorbent dosage, 0.5 mg/ml; t, 24 hours; and T, 303 K.

Gibbs free energy change is given by Eq. 7. The combination of Eqs. 6 and 7 gives the van't Hoff equation (Eq. 8).

$$\Delta G = \Delta H - T\Delta S \quad (7)$$

$$\ln K_c = \frac{-\Delta G}{RT} = \frac{\Delta S}{R} - \frac{\Delta H}{RT} \quad (8)$$

where T is the absolute temperature (K) and R is the universal gas constant (8.314 J/mol.K). The values of thermodynamic parameters determined at different temperatures are tabulated in Table 3. The sorption performance of PAL sorbents was found to decrease with increasing temperature. The ΔG values of M-LA-PAL and M-SA-PAL sorbents were negative and increases with temperature indicating a decrease in the spontaneity and feasibility of sorption at a higher temperature. In general, the ΔG for physisorption is in a range of -20 to 0 kJ/mol while the chemisorption varies between -80 to -400 kJ/mol. The ΔG for M-LA-PAL and M-SA-PAL varies from -5.304 to -2.974 kJ/mol over the temperature studied, indicating that the physisorption took place in the sorption process. Conversely, the ΔG obtained for R-PAL is positive, which meant the sorption process is non-feasible and non-spontaneous at the studied temperature. However, the ΔH and ΔS are negative values, revealing that the sorption was feasible for R-PAL at lower temperature [36]. The negative values of ΔH for the PAL sorbents reveal that the sorption is exothermic and had more possibilities to be controlled by physical processes in nature involving weak forces of attraction [37]. The negative value of ΔS indicates an increase in randomness in the solid/solution interface and oil molecules were orderly sorbed onto PAL surfaces [36].

The minimum kinetic energy needed by the sorbate molecules to react with the active sites available on the surface of sorbent is defined as the activation energy, E_a (kJ/mol). The value of E_a can be determined from the Arrhenius equation (Eq. 9).

$$lnk_2 = \ln A - \frac{E_a}{R}\left(\frac{1}{T}\right) \quad (9)$$

where k_2 is the pseudo-second order rate constant at a different temperature, A is the Arrhenius constant and R is the gas constant (8.314 J/mol/K). The type of sorption (physisorption or chemisorption) can be identified from the magnitude of E_a calculated. It was reported that E_a of 5-40 kJ/mol is due to physisorption while E_a of 40-800 kJ/mol is given by chemisorption [8,36]. In physisorption, equilibrium is attained rapidly and easily reversible as the forces involved are weak while chemisorption is specific and the forces involved are much stronger than in physisorption [38]. The calculated E_a obtained was 10.74, 14.18 and 23.67 kJ/mol for R-PAL, M-LA-PAL and M-SA-PAL, respectively and these imply that the sorption of oil molecules onto PAL surfaces is physisorption. These results are basically in agreement with the value of ΔG and ΔH, which confirmed that the physisorption takes place in the oil sorption onto PAL sorbents. Sidik et al. also reported that the physisorption took place in the removal of dispersed crude oil by modified oil palm leaves[8].

3.7 Effect of contact time

Sorption is a time dependent process and it is crucial to know the rate of sorption for designing and evaluating the sorbent performance in oil removal. The kinetics of oil sorption onto R-PAL and fatty acid esterified PAL (M-LA-PAL and M-SA-PAL) sorbents at various temperatures is presented in Fig. 7(a). It was found that the sorption rate was rapid at the first few hours, then proceeded at a slower rate and finally attained equilibrium sorption at 9 hours (540 minutes). The fast phase sorption may be due to the sorption by the external surface area or the fiber pores whereas the slower rate is

Journal Name

ARTICLE

Table 2. Isotherm model analysis of PAL sorbents.

Isotherm	Parameters	Values		
		R-PAL	M-LA-PAL	M-SA-PAL
Langmuir	q_m (mg/g)	62.50	181.82	204.08
	K_a (L/mg)	0.0256	0.1285	0.3043
	R^2	0.9417	0.9958	0.999
	χ^2	6.987	21.588	24.24
Freundlich	K_F (mg/g)(L/mg)$^{1/n}$	2.5060	36.162	21.815
	n	1.5342	3.3967	2.1988
	R^2	0.8674	0.9796	0.8302
	χ^2	20.087	14.775	86.79
Temkin	A (L/g)	0.345	35.703	1.5541
	b_T (J/mol)	N/A[C]	N/A[C]	N/A[C]
	R^2	0.9311	0.84	0.9741
	χ^2	5.100	32.567	5.4786

Table 3. Temperature dependence thermodynamic parameters analysis.

Temperature (K)	q_e (mg/g)	ΔG (kJ/mol)	ΔH (kJ/mol)	ΔS (kJ/mol.K)	Ea (kJ/mol)
R-PAL					
303	35.59	2.908	-2.0043	-0.0756	10.74
323	26.92	4.422			
343	17.74	5.974			
M-LA-PAL					
303	107.67	-3.180	-11.021	-0.0259	18.34
323	103.32	-3.164			
343	95.48	-2.974			
M-SA-PAL					
303	138.89	-5.304	-14.981	-0.0319	23.67
323	120.69	-4.666			
343	111.85	-4.030			

probably associated with the diffusion of the sorbate in the inner part of the fiber micropores[39]. The sorption capacities of PAL sorbents were found to decrease when the temperature was increased. The highest sorption capacity obtained at 303 K was 35.59, 107.67 and 138.89 mg/g for the R-PAL, M-LA-PAL and M-SA-PAL, respectively.

The time dependence of sorption data was further analyzed assuming that the mechanism of oil sorption can generally be described by four consecutive rate controlling steps namely external mass transfer (transport from the bulk solution to the sorbent surface), film diffusion (diffusion across the liquid film from the sorbent surface), intraparticle diffusion (pore diffusion, surface diffusion or combination of both mechanisms), and surface interaction on sorbent active sites. The diffusional model was derived by assuming (i) intraparticle diffusion occurs by pore volume diffusion (Fick diffusion) and surface diffusion, (ii) the rate of sorption on the active site is instantaneous, and (iii) sorbent particles are spherical [40].

It is commonly known that the sorption process is the rate-controlled process in which the slowest step determines the process rate limiting step. At most of the time, only film and intraparticle diffusions are considered as rate limiting steps as the external mass transfer and surface chemical interaction processes are rapid. The rate limiting step of the sorption can be qualitatively determined by analyzing kinetic data using the Weber-Morris model as given by Eq. 9[41,42].

$$q_e = k_i\, t^{0.5} + C \qquad (9)$$

where k_i is the diffusion coefficient (mg/g/min$^{0.5}$) and C is a constant that gives an indication of the thickness of boundary layer. The sorption process is said to be intraparticle diffusion controlled if the straight line plot passes through the origin while the boundary layer diffusion (external mass transfer or film diffusion) may take place if it does not pass through the origin[41]. Fig. 7(b) shows that the plot of R-PAL passes through the origin, while M-LA-PAL and M-SA-PAL did not pass through the origin. A three-stage multi-linear

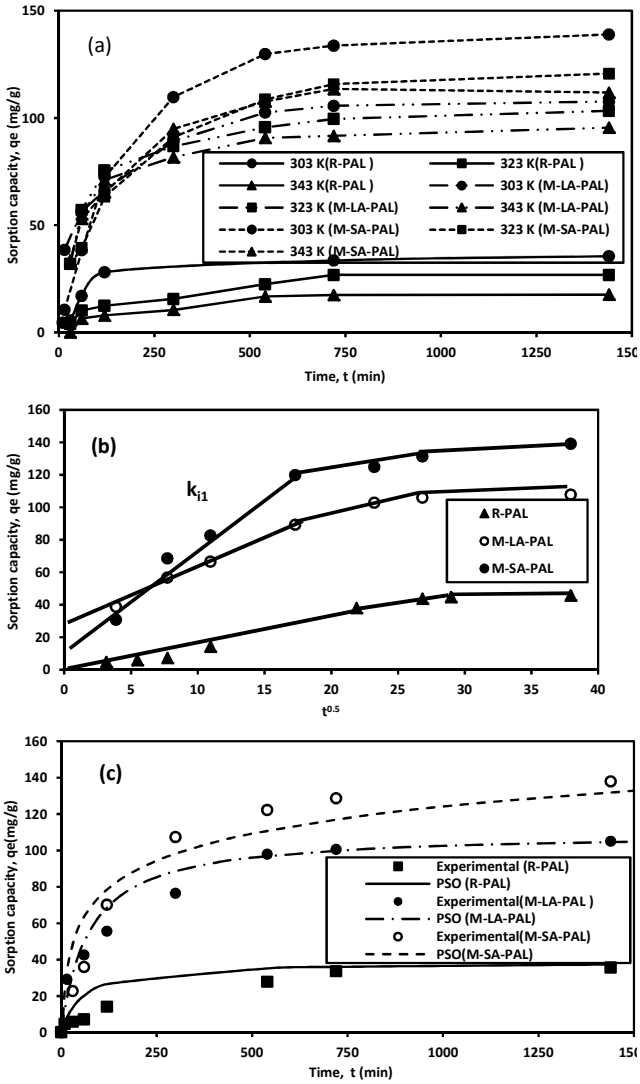

Fig. 7 Kinetics of oil sorption onto PAL sorbents: (a) sorption time dependence, (b) intraparticle/Weber Morris plots of oil sorption kinetic data and (c) surface chemical interaction model analysis. Experimental conditions: pH, 7; oil concentration, 100 ppm; sorbent dosage, 0.5 mg/mL; t, 0.5-24 hours and T, 303-343 K.

sorption process represents: (a) 1st stage (k_{i1}) was attributed to the boundary layer diffusion of the sorbate molecules; (b) 2nd stage (k_{i2}) was the gradual intraparticle diffusion and (c) 3rd stage (k_{i3}) was attributed to the final equilibrium of sorption process. The Weber-Morris model gives only the early understanding about diffusion mechanism. In order to confirm the rate limiting step of the diffusion process, the film diffusion and intraparticle coefficient need to be determined from Fick's law model and Boyd's plot, respectively.

During the film diffusion, a fictitious laminar boundary film is formed near to the sorbent surface in which the solute diffuses across it. By considering other diffusions are absent, the solute film diffusivity, D_f (cm^2/min) can be calculated by using the Fick's law model developed by Crank as given by Eq. 10[43,44].

$$\frac{q_t}{q_e} = 6\left(\frac{D_f}{\pi R_p^2}\right)^{0.5} t^{0.5} \quad (10)$$

where q_t and q_e respectively represent the sorption capacity at any time t and equilibrium (mg/g), and R is the sorbent particle radius (m). The D_f value was calculated from the initial slope of kinetic data and tabulated in Table 4. It was found that the M-SA-PAL gave the highest calculated D_f value, followed by M-LA-PAL and R-PAL at temperature of 303 – 343 K. The D_f value decreased as the temperature increased due to the greater internal energy of oil molecules.

The intraparticle diffusion occurs right after the film diffusion step. It involves the solute diffusing into the sorbent pores to the internal sorbent surface active sites. The intraparticle diffusion is usually dependent on the sorbent particle size, sorbate initial concentration and solid-fluid ratio (sorbent dosage) of the system[45,46]. It comprises of pore diffusion (D_p) and surface diffusion (D_s) in which the combination of both diffusions is expressed as an effective diffusivity, D_{eff} (m^2/min). Previously, there were several models developed to study the intraparticle diffusivity, namely film-pore diffusion model, pore volume diffusion model, pore volume and surface diffusion model and surface diffusion model by a numerical method (based on the tortuosity factor (τ)) and an analytical method (by minimizing the error (ARE)) between the experimental time and the calculated time from the sorption model)[47,48]. However, the Boyd's plot was used in this study rather than the above methods as it is simple and gives satisfactory results. By neglecting the effect of film diffusion, the effective diffusivity, D_{eff} (m^2/min) can be calculated by using Eqs. 11-14:

$$F = 1 - \frac{6}{\pi^2}\sum_{n=1}^{\infty}\frac{1}{n^2}\ exp\ \left(-\frac{n^2\pi^2 D_{eff} t}{R^2}\right) \quad (11)$$

$$F = 1 - \frac{6}{\pi^2}\sum_{n=1}^{\infty}\frac{1}{n^2}\ exp\ \left(-n^2 Bt\right) \quad (12)$$

where $F = q_t/q_e$ is the fractional attainment of equilibrium at time t (min), B is the time constant (min^{-1}) and R is the radius of the sorbent particle. The D_{eff} can be determined from the Boyd's plot (Bt versus time) in which the Bt can be expressed by Eqs. 13 and 14:

F values > 0.85 $$Bt = -0.4997 - \ln(1 - F) \quad (13)$$

F values < 0.85 $$Bt = \left(\sqrt{\pi} - \sqrt{\pi - \frac{\pi^2 F}{3}}\right)^2 \quad (14)$$

The slope of the Boyd's plot (S) is given by Eq. 15, from which the D_{eff} value was then calculated and tabulated in Table 4.

$$S = \frac{\pi^2 D_{eff}}{R^2} \quad (15)$$

Similar to the film diffusion study, the D_{eff} of PAL sorbents at any temperature follow the order M-SA-PAL> M-LA-PAL>R-PAL (Table 4). The D_{eff} was also found to decrease as observed for the D_f with the increase of the sorption temperature. Since the film diffusion coefficient (D_f) obtained was found to be lower than D_{eff}, thus, the film diffusion was identified as the rate limiting step of the oil sorption onto R-PAL, M-NBS-PAL and M-SA-PAL sorbents.

The surface chemical interaction between solute and sorbent surface active sites can be either physical (physisorption), chemical (chemisorption) or a combination of both depending on the interaction forces involved. Several chemical reaction kinetic models have been reported to describe these interactions and the

most widely used chemical reaction kinetic models are pseudo-first order (Lagergren model), pseudo-second order (Ho and Mckay model) and Elovich models. The pseudo-first order (PFO) equation is generally applicable over the initial stage of the adsorption process whereas pseudo-second (PSO) order equation predicts the behavior over the whole range of adsorption. The PFO assumes that the sorption is a pseudo-chemical reaction and the rate of occupation of binding sites is proportional to the number of the unoccupied sites of the sorbent.

The PSO model also assumes the sorption is a pseudo-chemical reaction and the rate of occupation of binding sites is proportional to the square of the number of unoccupied sites on the sorbent surface. The Elovich kinetic model is generally applicable to the chemisorption kinetics whereby active sites are heterogeneous in nature and therefore, exhibit different activation energies for chemisorption. This model was originally developed to describe the kinetics of heterogeneous chemisorption of gases onto solid surfaces but it is later used in soil chemistry generally to describe the kinetics of sorption and desorption of different types of inorganic materials on soils [49]. The PFO, PSO and Elovich kinetic models can be expressed in the linear form as shown in Eqs. 16-18, respectively.

$$\log(q_e - q_t) = \log q_e - \frac{k_1 t}{2.303} \quad (16)$$

$$\frac{t}{q_t} = \frac{1}{k_2 q_e^2} + \frac{t}{q_e} \quad (17)$$

$$q_t = q_o + \frac{1}{\beta}\ln(\alpha\beta) + \frac{1}{\beta}\ln t \quad (18)$$

where q_o, q_t and q_e are respectively the sorption capacities (mg/g) at initial (t = 0), time t (minutes) and equilibrium, k_1 (g/mg/min) and k_2 (g/mg/min) are respectively the rate constants of the pseudo-first order and pseudo-second order kinetic models, α is the initial sorption rate (mg/g/min), and β is the desorption constant (mg/g/hr).

The coefficient of determination (R^2), Pearson's chi-squared test (χ^2) analysis and model parameter constants were calculated and given in Table 5. The non-linear plot of the best fitting model using parameters obtained from the linear fitting for the kinetic data of PAL sorbents is shown in Fig. 7(c). For the entire sorption process, it shows that the PSO kinetic model gave the highest R^2 and lowest χ^2 values for the PAL sorbents studied compared to the PFO and the Elovich model. The kinetic data generated from the PFO and PSO fitted the experimental data reasonably well and $q_{e,\,calc}$ values were also close to $q_{e,\,exp}$. However, the Elovich model shows poor fitting with the experimental data, lowest R^2 and highest χ^2 values. Thus, the PSO kinetic model is much better than PFO and Elovich model in interpreting the sorption behavior of oil sorption onto R-PAL, M-LA-PAL and M-SA-PAL after all the criteria were taken into consideration. This indicates that chemisorption takes place in the sorption of oil onto PAL sorbents.

The kinetics of the process can thus be controlled by either diffusion or chemical step which can be determined by analyzing the E_a calculated from the Arrhenius equation by plotting the diffusion coefficient (k_{i1}) of the Weber–Morris against the reciprocal

Table 4 The calculated external mass transfer coefficient, film and effective diffusivities of PAL sorbents at 303-343 K.

		Sorbents		
	Temperature (K)	**R-PAL**	**M-LA-PAL**	**M-SA-PAL**
Effective diffusivity,	303	6.410	13.10	16.03
D_{eff} (x10^{13} m^2/min)	323	3.526	12.20	11.86
	343	3.206	9.91	10.26
Film diffusivity,	303	3.080	5.6	6.8
D_f (x10^{13} m^2/min)	323	2.552	5.5	6.7
	343	2.507	5.0	5.5

Table 5 Kinetic model analysis of PAL sorbents.

	Sorbents		
	R-PAL	**M-LA-PAL**	**M-SA-PAL**
$q_{e,\,exp}$ (mg/g)	35.59	107.67	138.89
Pseudo-first order (PFO)			
k_1(g/mg/hr)	0.0668	0.0062	0.0076
$q_{e,\,calc}$ (mg/g)	38.64	128.85	256.51
R^2	0.8926	0.9612	0.9095
χ^2	95.8295		
Pseudo-second order (PSO)			
k_2x10^3 (g/mg/hr)	10.482	0.127	0.0716
$q_{e,\,calc}$ (mg/g)	38.7597	109.89	131.58
R^2	0.9724	0.9929	0.9874
χ^2	20.8052		
Elovich			
α (mg/g/min)	65.6011	8.5313	6.9359
β (g/mg)	0.08244	0.0644	0.0465
R^2	0.9299	0.9521	0.8751
χ^2	34.8452		

temperature [41]. The energy of diffusion controlled sorption process is usually less than 25-30 kJ/mol while for energy higher than 25-30 kJ/mol is normally chemical (activation) controlled process. The calculated E_a values of R-PAL, M-LA-PAL and M-SA-PAL were found to be 11.338, 8.443 and 8.183 kJ/mol respectively, indicating that the sorption process was controlled by the diffusion process. The film diffusion was thus confirmed as the rate limiting step of the oil sorption whereby the natural interaction at the surface active sites was physisorption for the entire PAL studied. The same results were also reported for dispersed oil sorption. [8]

3.8 Oil sorption mechanism

The mechanism of oil sorption by natural fibers can be either through absorption, capillary action, adsorption and/or a combination of these processes. The esterified PAL sorbents may have the same mechanism as flax as both sorbents have hydrophobic and oleophilic features on the surface [50]. Thus, the mechanism of oil sorption onto esterified PAL sorbents can be the combination of adsorption by interaction of hydrophobic surface and oil, adsorption of fibers that have irregular surface morphology, and capillary action by diffusion of oil into the sorbent (as a result of concentration gradient and the capillary pressure existing in the sorbent pores). Since esterified PAL sorbent is cellulosic fiber, the oil sorption of PAL sorbents by absorption into the pores may be assumed to be neglected [50].

The oil sorption process on surface active sites may involve physical, chemical and/or a combination of both phenomena. The physical phenomenon involves the transport of oil molecules from the bulk solution to the sorbent surfaces, while the chemical phenomenon involves the interactions of oil molecules with sorbent surfaces which are either through physical or chemical interactions and/or a combination of both interactions. The sorption time needed by PAL sorbents in order to reach equilibrium is about 9 hours. The long sorption time denotes the slow external and intraparticle diffusion of oil molecules. The rapid phase at the early sorption stage is due to the sorption by the external area or fiber pores whereas the slow phase is probably due to the diffusion of oil into the inner part of the fiber micropores [39]. The calculated Ea value using the diffusion coefficient (k_{i1}) of Weber–Morris indicates that the oil sorption process was controlled by the diffusion process and the film diffusion was confirmed as the rate limiting step based on the diffusion analyzes which have been discussed previously.

The sorbate interaction at the sorbent surface active sites can be distinguished into physisorption, chemisorption and ion-exchange processes. Physisorption normally happened at a lower temperature and is characterized by a relatively low energy of sorption. It occurs due to the van der Waals forces of attraction, which also means that the sorbate is not held strongly to the sorbent. Chemisorption is characterized by a high energy of sorption and favored at a higher temperature. It involves valence forces through the sharing or exchange of electrons between sorbent and sorbate and thus the chemisorbed molecules are held together by a strong localized bonds[51]. Ion-exchange involves the exchange between ions of the substance concentrate at the surface due to the electrostatic attraction and solute in the bulk solution [52]. As discussed in the previous section, the sorption enthalpy of oil by R-PAL, M-LA-PAL and M-SA-PAL sorbents were 10.74, 14.18 and 23.67 kJ/mol which were in the range of 5-40 kJ/mol. These results suggest that the physical interaction (physisorption) took place in the sorption process. On the contrary, the results of surface chemical interactions data analysis indicated that the chemisorption played a role in the dissolved oil sorption process too.

The characteristics of sorbents also affect the sorption performance. The oil sorption capacity of natural fibers depends mostly on the surface void ratio and the surface composition of the fibers [53]. Thus, in this case, the presence of active sites and functional groups on the sorbents is needed in order to attach the oil molecules onto the PAL sorbents. Many researchers reported that sorbents with hydrophobic and oleophilic properties are more favorable for oil removal processes [18,50]. Due to this, the mercerization was conducted to increase the active sites available and then followed by esterification to attach the more hydrophobic and oleophilic long chain hydrocarbon groups onto the sorbent surface to enhance the sorption performance. The effect of the modifications is proven with the addition of a peak at ~1750 cm^{-1} which corresponds to the carbonyl group originated from the fatty acid. Besides, the broad band intensity observed at ~3440 – 3252 cm^{-1} due to the intermolecular hydrogen bonding was also reduced indicating that the hydroxyl groups in R-PAL were replaced by the acyl groups from the fatty acids. The effect of fatty acid esterification can also be proven by the results obtained from the XPS analysis as shown in Figs. 4(a) and 4(b). From the total C_{1s} high resolution spectra, C4 (O-C=O) appeared in the esterified PAL sorbents and the peak intensity for C_{1s} increased in the PAL sorbents after the esterification process as the acyl group from fatty acid was introduced into the PAL sorbent. It was confirmed by the increase in peak intensity of the total O_{1s} high resolution spectra after the sorbents modification.

The crude oil consists of various types of hydrocarbons which have different affinity to be sorbed onto the sorbent surfaces. Fig. 8 shows the crude oil compositions: (a) crude oil; (b) crude oil in water before sorption, crude oil in water after sorption by (c) M-LA-PAL and (d) M-SA-PAL sorbents. These results show that the crude oil comprises of both short and long chain (C_6 to C_{23}) hydrocarbons as shown Fig. 8(a). There were only C_7 to C_{13} hydrocarbons being detected in the oil in water solution which represents the dissolved hydrocarbons such as benzene, toluene, ethylbenzene, xylene (BTEX) and alkyl naphthalene [54]. After the sorption by PAL sorbents, the peak number and peak abundance were reduced and this proved that certain hydrocarbon compounds were sorbed by sorbents during the sorption process. These results indicate that the removal performance decreased with decreasing carbon chain of hydrocarbon compounds. This supports the fact that the dispersed oil has a better removal performance than the dissolved oil contaminant.

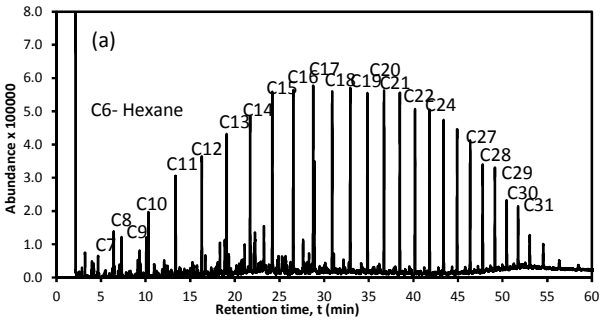

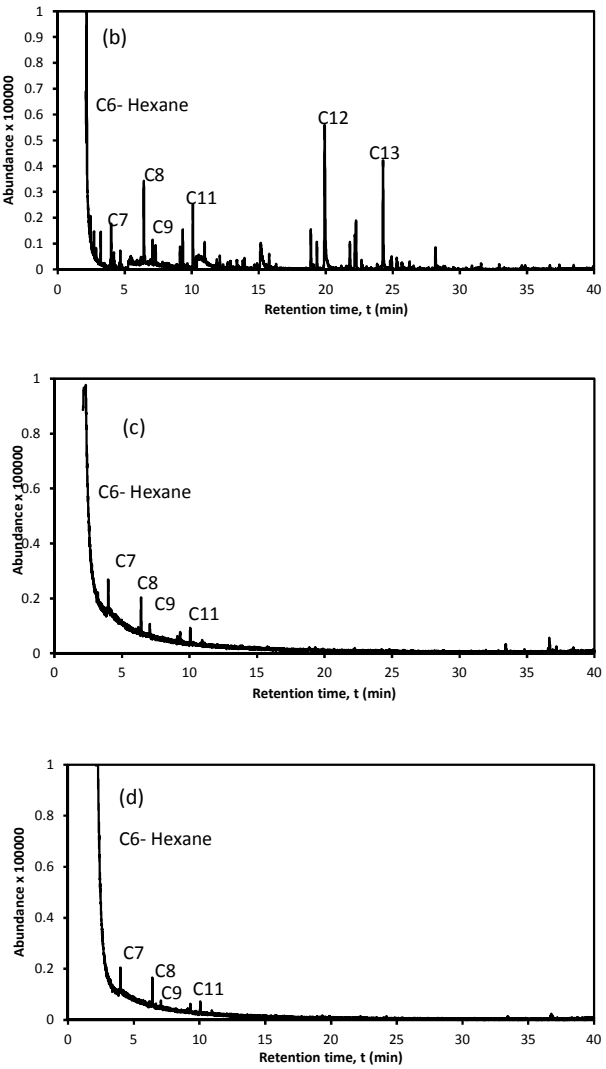

Fig. 8 The crude oil compositions: (a) crude oil; (b) crude oil in water before sorption, crude oil in water after sorption by (c) M-LA-PAL and (d) M-SA-PAL sorbents.

3.9 Regeneration analysis

A regeneration study was conducted to demonstrate the reusability of the sorbent. The sorbent has to be reusable in order to save the operating cost. In the current study, the regeneration process was conducted up to 4 cycles, which was enough to demonstrate the reusability performance of the sorbent as illustrated in the literature. The study was conducted on M-LA-PAL and M-SA-PAL, which had better performance than R-PAL. The sorbents were first loaded with crude oil and then the crude oil loaded sorbent was desorbed using isopropanol-water (1:1) solution. The oil sorption capacity with respect to the number of regeneration cycles is given in Fig. 9. The sorption capacity of M-LA-PAL and M-SA-PAL was 118.4 and 132.9 mg/g, respectively for freshly prepared sorbents. After regeneration, the oil sorption capacity of M-LA-PAL and M-SA-PAL for the second cycle reduced by ~5.20 % and ~7.44 %, respectively. The sorbent sorption capacity after four cycles decreased of 12.9 and 17.2 % for M-LA-PAL and M-SA-PAL, respectively. The results show that the repeated washed M-LA-PAL and M-SA-PAL can be used up to 4 continuous cycles without a drastic drop of sorption capacity. The oil sorption capacity decreasing with the increasing cycle number might be due to the incomplete desorption of oil molecules and led to some oil molecules still retained on the sorbent surface after the sorption. Besides, sorption capacity decrease may also be due to the bleach of carbonyl functional group into the desorbing solution during the desorption process. This study shows that M-LA-PAL and M-SA-PAL sorbents can be regenerated and reused repeatedly at least for four times. The comparison of maximum oil sorption capacity of crude oil on various sorbents is shown in Table 6. Due to the different oil-in-water systems used in the previous and the current study, the results were difficult to compare. Thus, the M-LA-PAL and M-SA-PAL were also used to sorb oil from the dispersed oil system according to the method proposed by Sidik *et al.* [8] and Sathasivam *et al.* [12]. The results show that the M-LA-PAL and M-SA-PAL performed better than lauric acid treated OPL, carbonized rice husks and fatty acid modified BTF [8,14,15]. These results show that the PAL fiber and thus lignocellulosic biomass could be potentially used economically as precursors in sorbent synthesis for the treatment of oil contaminated wastewater such as produced water from the oil and gas exploration activities.

Table 6 Sorption capacity of various sorbents.

Oil-in-water (o/w) system	Sorbent	Sorption capacity, q_e (g/g)	Oil concentration (ppm)	Reference
Dissolved oil	M-LA-PAL	0.108±0.004	100	This study
	M-SA-PAL	0.138±0.002	100	This study
Dispersed oil	M-LA-PAL	1.860±0.170	5000	This study
	M-SA-PAL	1.920±0.170	5000	This study
	M-LA-PAL	8.230±1.400	66667	This study
	M-SA-PAL	8.480±2.000	66667	This study
	Lauric acid treated oil palm leaves (OPL)	1.200±0.120	5600	Sidik *et al.*[6]
	Carbonized rice husks	6.000	-	Kumagai *et al.*[13]
	Fatty-acid modified banana trunk fibers (BTF)	8.000	66667	Sathasivam *et al.* [12]

Journal Name

ARTICLE

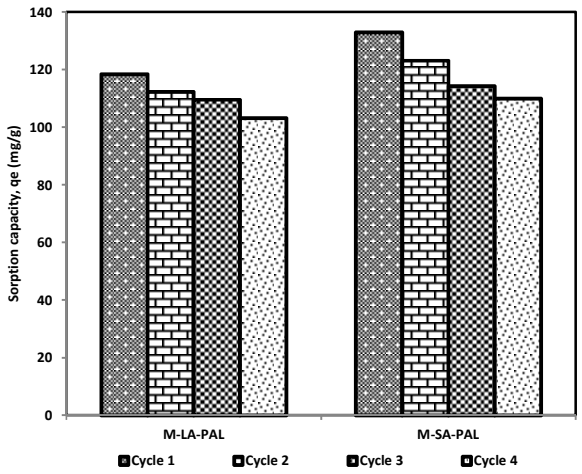

Fig. 9. Regeneration of M-LA-PAL and M-SA-PAL.

4. Conclusions

Lignocellulosic biomass of pineapple leaves (PAL) was used as a precursor in a dissolved oil sorbent synthesis. The PAL was first mercerized followed by esterification with fatty acids to modify the surface chemistry and thus enhance the dissolved oil sorption performance. The sorption performance of the PAL sorbents follow the order M-SA-PAL> M-LA-PAL> R-PAL which is lower than the dispersed oil sorption. The sorption data analysis indicates that the oil sorption onto PAL sorbents obeyed the Langmuir isotherm and pseudo-second order (PSO) kinetic models. The experimental evidence indicates that the oil removal from dissolved oil-in-water (o/w) solution was controlled by a physical phenomenon with the film diffusion as the rate-limiting step which is also similar to those results previously reported for dispersed o/w sorption studies. The regeneration results show that the synthesized PAL sorbents can be regenerated and reused repeatedly at least for four times. These results indicate that lignocellulosic biomass such as PAL could potentially be used as sorbent precursors not only for the removal of oil but might be also for other organic components from wastewaters. The conversion of lignocellulosic biomass to high value-added products such as sorbents could provide the economic benefits and also reduce the potential risk of environmental pollution.

Acknowledgements

The financial supports from the Ministry of Higher Education (MOHE), Malaysia for the MyBrain15 scholarship and the Universiti Teknologi Malaysia, Malaysia for the Research University Grants (GUP Grant Nos. 00H63 and 06H85) are gratefully acknowledged.

References

1 O. Rattanawong, L. Kaewsichan, N. Grisdanurak and A. Yuasa, *Korean J. Chem. Eng.*, 2007, **24**, 67–71.

2 A. Fakhru'l-Razi, A. Pendashteh, L. C. Abdullah, D. R. A. Biak, S. S. Madaeni and Z. Z. Abidin, *J. Hazard. Mater.*, 2009, **170**, 530–51.

3 J. Wang, Y. Zheng and A. Wang, *J. Environ. Sci. (China)*, 2013, **25**, 246–253.

4 A. Fakhru'l-Razi, A. Pendashteh, L. C. Abdullah, D. R. A. Biak, S. S. Madaeni and Z. Z. Abidin, *J. Hazard. Mater.*, 2009, **170**, 530–551.

5 A. Torabian, H. Kazemian, L. Seifi, G. N. Bidhendi, A. A. Azimi and S. K. Ghadiri, *Clean - Soil, Air, Water*, 2010, **38**, 77–83.

6 G. Deschamps, H. Caruel, M. E. Borredon, C. Bonnin and C. Vignoles, *Environ. Sci. Technol.*, 2003, **37**, 1013–1015.

7 A. R. Tembhurkar and R. Deshpande, *J. Hazardous, Toxic, Radioact. Waste*, 2012, **16**, 311–315.

8 S. M. Sidik, A. A. Jalil, S. Triwahyono, S. H. Adam, M. A. H. Satar and B. H. Hameed, *Chem. Eng. J.*, 2012, **203**, 9–18.

9 W. Zhang, H. Li, X. Kan, L. Dong, H. Yan, Z. Jiang, H. Yang, A. Li and R. Cheng, *Bioresour. Technol.*, 2012, **117**, 40–47.

10 C. Vaca-Garcia, S. Thiebaud, M. E. Borredon and G. Gozzelino, *J. Am. Oil Chem. Soc.*, 1998, **75**, 315–319.

11 N. Lopattananon, K. Panawarangkul, K. Sahakaro and B. Ellis, *J. Appl. Polym. Sci.*, 2006, **102**, 1974–1984.

12 A. R. Bertoti, S. Luporini and M. C. A. Esperidião, *Carbohydr. Polym.*, 2009, **77**, 20–24.

13 J. Wang, Y. Zheng and A. Wang, *Ind. Crops Prod.*, 2012, **40**, 178–184.

14 K. Sathasivam and M. R. H. Mas Haris, *Water. Air. Soil Pollut.*, 2010, **213**, 413–423.

15 S. Kumagai, Y. Noguchi, Y. Kurimoto and K. Takeda, *Waste Manag.*, 2007, **27**, 554–561.

16 N. Ali, M. El-Harbawi, A. A. Jabal and C. Y. Yin, *Environ. Technol.*, 2012, **33**, 481–486.

17 X. F. Sun, R. C. Sun and J. X. Sun, *J. Mater. Sci.*, 2003, **38**,

3915–3923.

18 L. Vlaev, P. Petkov, A. Dimitrov and S. Genieva, *J. Taiwan Inst. Chem. Eng.*, 2011, **42**, 957–964.

19 M. Husseien, A. A. Amer, A. El-Maghraby and A. Taha, *Int. J. Environ. Sci. Technol.*, 2009, **6**, 123–130.

20 S. Ibrahim, H. M. Ang and S. Wang, *Bioresour. Technol.*, 2009, **100**, 5744–5749.

21 N. A. Lutpi, in *Proceedings of the 3rd (2011) CUTSE International Conference*, 2011, pp. 8–9.

22 S. Neupane, S. T. Ramesh, R. Gandhimathi and P. V. Nidheesh, *Desalin. Water Treat.*, 2014, **54**, 2041–2054.

23 C. H. Weng, Y. T. Lin and T. W. Tzeng, *J. Hazard. Mater.*, 2009, **170**, 417–424.

24 B. H. Hameed, R. R. Krishni and S. A. Sata, *J. Hazard. Mater.*, 2009, **162**, 305–311.

25 P. Jandura, B. V. Kokta and B. Riedl, *J. Appl. Polym. Sci.*, 2000, **78**, 1354–1365.

26 A. R. Sena Neto, M. A. M. Araujo, F. V. D. Souza, L. H. C. Mattoso and J. M. Marconcini, *Ind. Crops Prod.*, 2013, **43**, 529–537.

27 N. E. Thompson, G. C. Emmanuel and K. J. Adagadzu, *Arch. Appl. Sci. Res.*, 2010, **2**, 142–151.

28 P. Garside and P. Wyeth, *Stud. Conserv.*, 2003, **48**, 269–275.

29 M. S. Huda, L. T. Drzal, A. K. Mohanty and M. Misra, *Compos. Interfaces*, 2008, **15**, 169–191.

30 A. Valadez-Gonzalez, J. M. Cervantes-Uc, R. Olayo and P. J. Herrera-Franco, *Compos. Part B Eng.*, 1999, **30**, 321–331.

31 L. M. Matuana, J. J. Balatinecz, R. N. S. Sodhi and C. B. Park, *Wood Sci. Technol.*, 2001, **35**, 191–201.

32 S. Ibrahim, S. Wang and H. M. Ang, *Biochem. Eng. J.*, 2010, **49**, 78–83.

33 M. Zhu, J. Yao, L. Dong and J. Sun, *Chemosphere*, 2016, **144**, 1639–1645.

34 H. H. Sokker, N. M. El-Sawy, M. A. Hassan and B. E. El-Anadouli, *J. Hazard. Mater.*, 2011, **190**, 359–365.

35 I. A. W. Tan, B. H. Hameed and A. L. Ahmad, *Chem. Eng. J.*, 2007, **127**, 111–119.

36 L. Abramian and H. El-Rassy, *Chem. Eng. J.*, 2009, **150**, 403–410.

37 V. Vimonses, S. Lei, B. Jin, C. W. K. Chow and C. Saint, *Chem. Eng. J.*, 2009, **148**, 354–364.

38 Z. Aksu and E. Kabasakal, *Sep. Purif. Technol.*, 2004, **35**, 223–240.

39 F. Aloulou, S. Boufi and J. Labidi, *Sep. Purif. Technol.*, 2006, **52**, 332–342.

40 R. Ocampo-Pérez, M. M. Abdel daiem, J. Rivera-Utrilla, J. D. Méndez-Díaz and M. Sánchez-Polo, *J. Colloid Interface Sci.*, 2012, **385**, 174–182.

41 Y. S. Ho, J. C. Y. Ng and G. McKay, *Sep. Purif. Rev.*, 2000, **29**, 189–232.

42 A. E. Ofomaja, *Bioresour. Technol.*, 2010, **101**, 5868–5876.

43 J. Crank, *The Mathematics of Diffusion*, Oxford University Press, Oxford, 1975.

44 G. L. Dotto and L. A. A. Pinto, *J. Hazard. Mater.*, 2011, **187**, 164–170.

45 V. K. Gupta and N. Verma, *Chem. Eng. Sci.*, 2002, **57**, 2679–2696.

46 C. F. Chang, C. Y. Chang, W. Höll, M. Ulmer, Y. H. Chen and H. J. Gross, *Water Res.*, 2004, **38**, 2559–2570.

47 K. K. H. Choy, J. F. Porter and G. McKay, *Chem. Eng. Sci.*, 2004, **59**, 501–512.

48 R. Ocampo-Perez, R. Leyva-Ramos, P. Alonso-Davila, J. Rivera-Utrilla and M. Sanchez-Polo, *Chem. Eng. J.*, 2010, **165**, 133–141.

49 D. L. Sparks, in *Soil Physical Chemistry, Second Edition*, ed. D. L. Sparks, CRC Press, 1999, pp. 135–191.

50 I. A. Ansari, G. C. East and D. J. Johnson, *J. Text. Inst.*, 2009, **94**, 1–15.

51 Y. S. Ho and G. McKay, *Process Biochem.*, 1999, **34**, 451–465.

52 S. Ayoob, A. K. Gupta and V. T. Bhat, *Crit. Rev. Environ. Sci. Technol.*, 2008, **38**, 401–470.

53 T. A. Dankovich and Y. Lo Hsieh, *Cellulose*, 2007, **14**, 469–480.

54 T. Utvic, *Chemosphere*, 1999, **39**, 2593–2606.

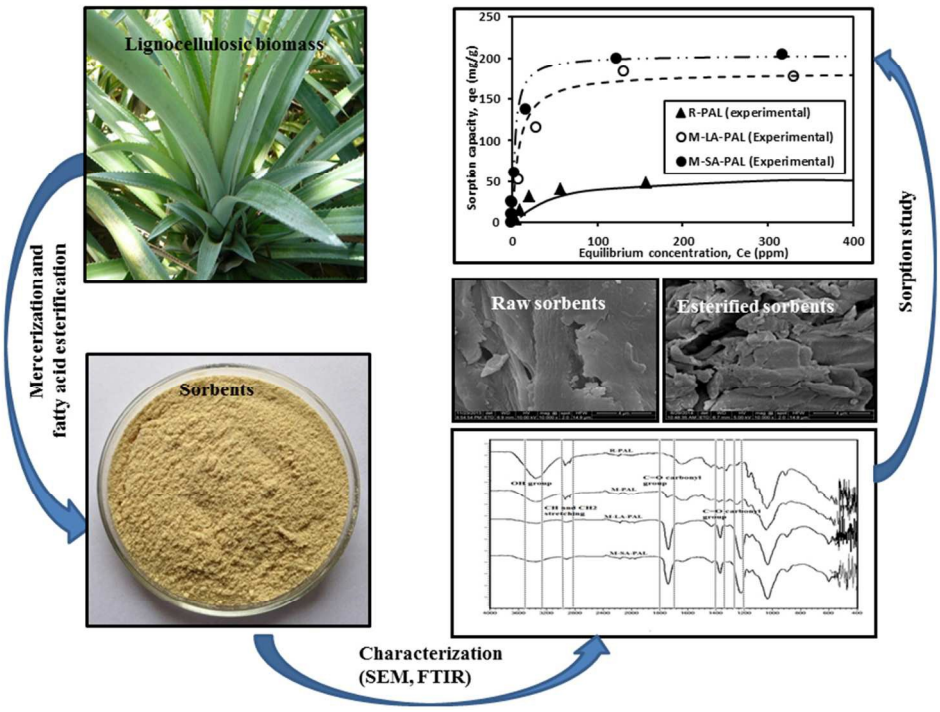

254x190mm (96 x 96 DPI)